Journal of Chromatography, 630 (1993) 37–52
Elsevier Science Publishers B.V., Amsterdam

CHROM. 24 685

Characterization of non-linear adsorption properties of dextran-based polyelectrolyte displacers in ion-exchange systems

Shishir D. Gadam, Guhan Jayaraman and Steven M. Cramer

Howard P. Isermann Department of Chemical Engineering. Rensselaer Polytechnic Institute, Troy. NY 12180-3590 (USA)

(First received June 11 th, 1992; revised manuscript received October 1st, 1992)

ABSTRACT

Experimental studies were carried out on the non-linear adsorption properties of dextran-based polyelectrolytes in anion- and cation-exchange chromatographic systems. By monitoring both the induced salt gradients and sequential breakthrough fronts, parameters were determined for use in a Steric Mass Action (SMA) model of non-linear ion-exchange chromatography. These parameters include: total ion capacity of the columns, characteristic charge, steric factor, equilibrium constant, and maximum adsorptive capacity for each of the polyelectrolytes. In addition the number of functional groups were determined by elemental analysis. The values of the SMA parameters were found to be independent of salt and polyelectrolyte bulk phase compositions. Parameters were also determined for a variety of proteins. Experimental isotherms for the polyelectrolytes and proteins were compared with those simulated by the SMA model. Finally, the implications of polyelectrolyte adsorption properties with respect to their ability to act as efficient displacers in ion-exchange displacement systems are discussed.

INTRODUCTION

The adsorption of polyelectrolytes at interfaces plays an important role in numerous industrial processes (e.g., colloid stabilization, emulsification, flocculation, drug delivery systems, chromatographic separations). Clearly, a fundamental understanding of polyelectrolyte adsorption behavior is critical for enhancing its successful application in these technologies.

The adsorption of charged macromolecules at interfaces depends on many variables (e.g., molecular mass, polyelectrolyte charge, surface charge, ionic strength and segment-segment interaction). Several theories of polyelectrolyte adsorption have been proposed in the literature [1–3]. These fundamental approaches are based on the lattice theory for adsorption of uncharged polymers developed by Roe [4] and Scheutjens and Fleer [5,6]. Adsorption of linear polyelectrolytes on highly charged surfaces are characterized by high-affinity isotherms, flat adsorbed layers and weak dependence upon molecular mass and salt concentration [2].

To date, relatively few studies have been carried out on the adsorption properties of polyelectrolyte displacers in chromatographic systems. Peterson and Torres [7,8] have employed frontal chromatography to determine the "number of bonds formed" between carboxymethyl dextrans and anionic chromatographic surfaces. Jen and Pinto [9] have examined the linear elution behavior of low-molecular-mass dextran sulphate. For relatively high-molecular-mass polyelectrolyte displacers ($M_r > 10\,000$) it is not feasible to determine the adsorption properties by linear elution techniques due to their high binding affinity and low desorption rates. Furthermore, measurement of steric effects in polyelectrolyte

Correspondence to: S. M. Cramer, Howard P. Isermann Department of Chemical Engineering, Rensselaer Polytechnic Institute, Troy, NY 12180-3590, USA.

0021-9673/93/$06.00

adsorption has not been reported in the chromatographic literature to date.

The steric mass action ion-exchange model (SMA) developed by Brooks and Cramer [10] explicitly accounts for steric effects in multicomponent protein equilibria and is able to predict complex behavior in ion-exchange displacement systems. Assuming that ion exchange is the only mechanism involved during adsorption, the stoichiometric exchange of the polyelectrolyte displacer and the exchangeable salt counter-ions can be represented by,

$$C_D + \nu_D \bar{Q}_s \Leftrightarrow Q_D + \nu_D C_s \quad (1)$$

where C and Q are the mobile and stationary phase concentrations, ν_D is the characteristic charge of the displacer, and subscripts D and s refer to the displacer and salt, respectively. The equilibrium constant is defined as,

$$K_D = \left(\frac{Q_D}{C_D}\right)\left(\frac{C_s}{\bar{Q}_s}\right)^{\nu_D} \quad (2)$$

Electroneutrality on the stationary phase requires

$$\Lambda \equiv Q_s + (\nu_D + \sigma_D) Q_D \quad (3)$$

where σ_D is the steric factor of the displacer.

The required model parameters for each component are: characteristic charge v, steric factor σ and equilibrium constant K. The characteristic charge represents the number of interactions between the adsorbent surface and a single macromolecule. The steric factor of a macromolecule represents the number of sterically hindered salt counter-ions on the adsorbent surface which are unavailable for exchange with other macromolecules in solution. The equilibrium constant is a measure of the affinity of the molecule. Earlier treatments of mass action ion-exchange equilibria assume that the binding of a macromolecule to the adsorbent surface only effects a number of adsorbent sites equal to its characteristic charge. As will be seen in this work, the steric shielding of the stationary phase sites plays an important role in the behavior of non-linear ion-exchange systems.

In order to employ this model for predicting the displacement behavior, it is critical that appropriate experimental protocols be developed for determining model parameters for the proteins and high-affinity polyelectrolyte displacers. In this manuscript, we will present experimental protocols for measuring SMA parameters of a variety of dextran-based polyelectrolyte displacers. The techniques presented here enable the determination of steric effects in polyelectrolyte adsorption along with the characteristic charge, equilibrium constant, and saturation binding capacity of the molecule in two sequential frontal experiments. In fact, this work has utilityforcharacterizinganynon-linearion-exchange adsorptive system. The parameters obtained in this manuscript are employed in the subsequent paper for simulating complex displacement behavior and investigating the effect of induced salt gradients in ion-exchange systems.

EXPERIMENTAL

Materials

Strong anion-exchange (SAX) (quaternary methyl amine, 8 μm, 50 x 5 mm I.D.) and cation-exchange (SCX) (sulphopropyl, 8 μm, 50 x 5 mm I.D.) columns were donated by Millipore (Waters Chromatography Division, Millipore, Milford, MA. USA). Tris-HCl and Tris buffer were purchased from Fisher Scientific (Springfield, NJ, USA). Sodium chloride, sodium nitrate, sodium monobasic phosphate, sodium dibasic phosphate and all proteins were purchased from Sigma (St. Louis, MO, USA). All dextran-based polyelectrolyte displacers were donated by Pharmacia-LKB Biotechnology (Uppsala, Sweden). Cellulose triacetate membranes (5000 and 10 000 molecular mass cut off) were obtained from Sartorius (Gbttingen, Germany). Reagent grade potassium chromate, silver nitrate and cesium chloride were obtained from Aldrich (Milwaukee, WI, USA). Polyvinylsulphuric acid potassium salt (PVSK), polydiallyl dimethyl ammonium chloride (polyDADMAC) and o-toluidine blue indicator were obtained from Nalco (Naperville, IL, USA).

Apparatus

Ultrafiltration of polyelectrolytes was carried out using an Amicon 8050 stirred cell (Amicon, Danvers. MA, USA). All frontal and elution chromatographic experiments were carried out with a modular chromatographic system consisting of a Model LC 2150 pump (LKB, Bromma, Sweden), a spectro-

flow 757 UV-Vis detector (Applied Biosystems, Foster City, CA, USA) and a Waters R401 differential refractometer. Data acquisition from the frontal experiments was carried out using Kipp and Zonen BD40 strip-chart recorder (Delft, Holland), and Waters Maxima 820 chromatographic workstation. Fractions of the column effluent were collected using an LKB 2212 Helirac fraction collector. Sodium ion analysis was performed using a Perkin-Elmer, Model 3030 (Perkin-Elmer, Norwalk, CT, USA) atomic absorption spectrophotometer. A 10-port valve Model C10W injector (Valco, Houston, TX, USA) with multiple loops was used to conduct all the frontal experiments. Lyophilization was carried out using a Model Lyph Lock 4.5 Freeze Dry System (Labconco, Kansas City, MO, USA).

Procedures

Purification of polyelectrolytes

All the polyelectrolyte displacers were ultraliltered as well as diafiltered to remove salts and other low-molecular-mass impurities. 5000 and 10 000 molecular mass cut off membranes were employed to purify the M_r 10 000 and 20 000–50 000 displacers, respectively. After ultrafiltration, the retentate was lyophilized.

Polyelectrolyte analysis

All polyelectrolytes were analyzed using a colloidal titration assay provided by Nalco Chemical Company. For analysis of dextran sulphates, a known volume of polyDADMAC reagent was added to the aqueous displacer solutions. Subsequent addition of o-toluidine indicator produced a colorimetric change. The excess polyDADMAC reagent was titrated against PVSK in presence of a *o*-toluidine indicator. For the analysis of DEAE–dextran the solution was titrated against PVSK without addition of the polyDADMAC reagent. Linear calibrations were obtained with both of these titrations.

Analyses for counter-ions

Chloride ion analysis. Chloride ion analysis was carried out using the ASTM assay [11]. For calibration, a known amount of chloride ion in 50 ml deionized water was titrated against 0.01 *M* silver nitrate using potassium chromate indicator solution. This technique was able to accurately monitor down to 10 μmol of chloride ion. A blank titration was performed to account for the chloride in water. The technique was able to selectively detect chloride ions in the presence of other salts, proteins, and displacers.

Sodium ion analysis. For the cation-exchange experiments, sodium was analyzed using atomic absorption spectrometry. Effluent fractions were diluted 3000-fold in plastic tubes containing 5 g/l cesium chloride solution (to minimize background noise) and their amounts quantitated against known Na^+ ion standards (10-50 μM).

Bed capacity measurements

Anion-exchange column. The capacity of the anion exchanger was measured in two different ways. The column was first perfused with 10 column volumes of 50 m*M* Tris–HCl buffer, pH 7.5. A front of 100 m*M* nitrate was then introduced and the column effluent was monitored at 310 nm. In addition, the column effluent'was collected for subsequent chloride analysis. The bed capacity was then determined from both the nitrate breakthrough front as well as the total amount of displaced chloride. The nitrate breakthrough technique is similar to that reported by Bentrop and Engelhardt [12].

Cation-exchange column. The cation exchanger was first equilibrated with 100 m*M* sodium phosphate buffer, pH 7.5, for approximately 10 column volumes followed by a front of 1 *M* ammonium sulphate. The column effluent was collected for subsequent sodium analysis. The bed capacity was then determined by measuring the amount of sodium ions displaced by the ammonium front.

Elemental analyses of dextran-based displacers

For each polyelectrolyte, the number of functional groups per molecule (e.g., sulphate and DEAE) were determined from sulphur and nitrogen elemental analysis. The elemental analyses were carried out by Galbraith Laboratories (Knoxville, TN, USA).

Determination of SMA parameters and induced salt gradients for polyelectrolyte displacers

Dextran sulphate in anion-exchange system. The following experimental protocol was employed for the chromatographic characterization of dextran sulphates:

(I) Stationary phase concentration: stationary phase concentrations of the dextran sulphate displacers were determined using frontal chromatography [13]. A 50 x 5 mm I.D. column was equilibrated with Tris buffer, pH 7.5, for approximately 10 column volumes. A front of dextran sulphate solution in the carrier was then introduced into the column at 0.2 ml/min and the column effluent was monitored at 252 nm to determine the breakthrough volume. The stationary phase concentration of the displacer, Q_D, was determined from the breakthrough volume, V_B, by

$$Q_D = \mathrm{CD}\ (V_B - V_0)/V_{sp} \quad (4a)$$

where C_D is the mobile phase concentration of polyelectrolyte displacer, V_0 is the dead volume of the column and V_{sp} is the column stationary phase volume. The number of moles of displacer adsorbed on the stationary phase, n_D, was calculated by

$$n_D = C_D\ (V_B - V_0) = Q_D\ V_{sp} \quad (4b)$$

(2) *Induced salt gradient:* during the frontal experiment, the column effluent was collected for subsequent chloride analysis. The induced salt gradient was then determined by measuring the total amount of chloride displaced, n_1, during the frontal experiment:

$$\Delta C_s = n_1/(V_B - V_0) \quad (5)$$

where ΔC_s is the step increase in the mobile phase counter-ion concentration upon displacer adsorption (Fig. 1).

(3) *Characteristiccharge:* thecharacteristiccharge of the displacer, ν_D, was determined from the induced salt gradient using the following expression:

$$\nu_{D,\mathrm{chloride}} = n_1/n_D = \Delta C_s/C_D \quad (6)$$

This approach for determining the characteristic charge from the induced salt gradient is depicted in Fig. 1.

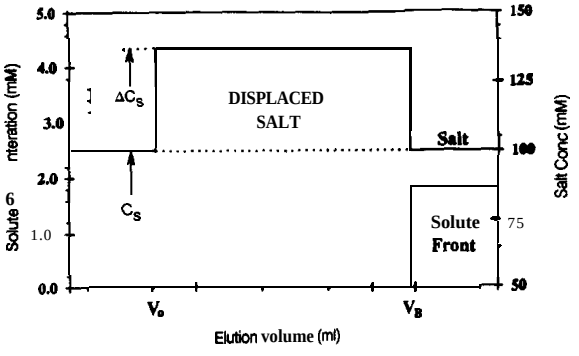

Fig. 1. Schematic of the induced salt gradient frontal chromatographic technique for determination of characteristic charge of polyelectrolytes.

(4) *Steric factor:* at sufficiently low mobile phase salt concentration the displacer completely saturates the stationary phase material. Frontal experiment under these conditions can be employed to determine the steric factor, σ_D, from the following expression [10]:

$$\sigma_D = (\Lambda/Q_D^{max}) - \nu_D \quad (7)$$

where Λ is the ion bed capacity and Q_D^{max} is the maximum stationary phase capacity of the polyelectrolyte displacer.

An independent direct measurement of steric factor can be carried out using a nitrate frontal experiment. A front of 100 mM sodium nitrate was perfused into a column saturated with the displacer. The column effluent was monitored at 310 nm to determine the nitrate breakthrough volume. Since the nitrate ions are small, they are able to access the sterically hindered chloride ions present on the surface and undergo ion exchange. The steric factor for the adsorbed displacer can then be determined from the nitrate breakthrough volume, $V_{B\text{-nitrate}}$, by

$$\sigma_{D,\mathrm{nitrate}} = C_{\mathrm{nitrate}}\ (V_{B\text{-nitrate}} - V_0)/n_D \quad (8)$$

where C_{nitrate} is the concentration of the nitrate front. In addition, the steric factor can be determined by measuring the chloride ion displaced by the nitrate front, n_2, as given by

$$\sigma_{D,\mathrm{chloride}} = n_2/n_D \quad (9)$$

In order to check the internal consistency of these methods, the characteristic charge of dextran sulphate can be independently calculated using the expression:

$$\nu_{D,\mathrm{nitrate}} = (\Lambda/Q_D^{max}) - \sigma_{D,\mathrm{nitrate}} \quad (10)$$

where, Q_D^{max} is determined by eqn. 4 under saturation conditions and $\sigma_{\mathrm{nitrate}}$ is determined by eqn. 8.

An example of this sequential chromatographic method for the 10 000 dextran sulphate displacer is presented in Fig. 2.

(5) *Equilibrium adsorption constant:* the equilibri-

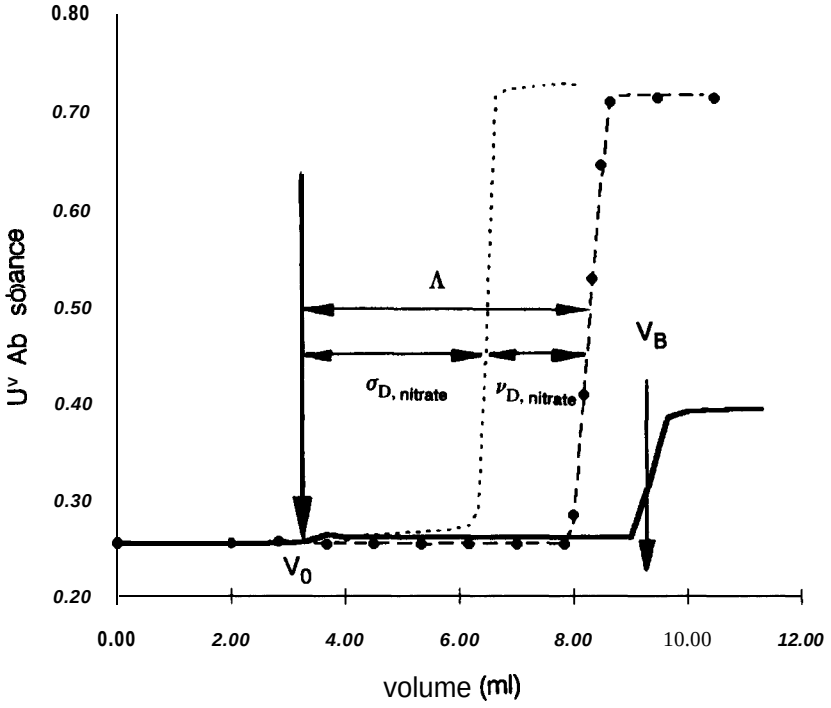

Fig. 2. Sequential frontal chromatographic protocol for determination of SMA parameters for dextran sulphate. Chromatographic conditions: nitrate fronts, 100 m*M* sodium nitrate; dextran sulphate front, 10 mg/ml in 50 m*M* Tris–HCl, pH 7.5. The horizontal arrows represent the elution volumes used to determine the corresponding model parameters. --- = Nitrate front (initial); ● = nitrate front (after regeneration); ——— = M_r10 000 dextran sulphate; ----- = nitrate front (saturated column).

urn constant for the ion-exchange process is defined in eqn. 3. Once the characteristic charge and steric factor are measured independently as described above, a frontal experiment was employed for the determination of the equilibrium constant K_D. This experiment was performed under elevated mobile phase salt conditions where the solute does not completely saturate the bed. The equilibrium constant was directly calculated from the breakthrough volume using the independently determined values of the characteristic charge (ν_D) and steric factor (an) by the expression [10]:

$$K_D = \frac{1}{\beta}\left(\frac{V_B}{V_0} - 1\right)\left(\frac{C_s}{\Lambda - (\nu_D + \sigma_D)\frac{C_D}{\beta}\left(\frac{V_B}{V_0} - 1\right)}\right)^{\nu_D} \quad (11)$$

where β is the column phase ratio and C_s is the initial salt concentration in the carrier.

At the end of these experimental procedures, the column was regenerated by passing five column volumes of 1.5 A4 NaCl solution in 100 m*M* phosphate buffer, pH 2.1, as the regenerant. The total ion bed capacity was then re-determined to ensure complete regeneration of the column.

DEAE-dextran in cation-exchange system. The experimental protocols for measuring the SMA parameters of DEAE–dextran displacers in the cation-exchange system were similar to those described above for the anion-exchange displacers. Mobile phases consisted of various concentrations of sodium phosphate buffer, pH 6.0. Column effluents were monitored using refractive index (RI) detection. Sodium ion content was determined using atomic absorption spectroscopy. The regenerant solution was 1 *M* NaCl in 100 m*M* phosphate buffer, pH 11.0.

Determination of SMA parameters for proteins

The SMA parameters for several proteins were

obtained according to the protocol described by Brooks and Cramer [IO]. Briefly, linear elution experiments were carried out at various mobile phase salt concentrations in order to determine the characteristic charge (ν_P) and equilibrium constant (K_P) by the following equations:

$$\log k' = \log (\beta K_P \Lambda^{\nu_P}) - \text{vp} \log C_s \quad (12)$$

where a plot of a log k' *vs. log* C_s yields a straight line with a slope of $-\nu_P$, and intercept of log $(\beta K_P \Lambda^{\nu_P})$. Linear elution data for β-lactoglobulin A and B were obtained on the SAX column using Tris chloride mobile phase. In the cation-exchange system, linear elution data were obtained for a-chymotrypsinogen A, cytochrome c, and lysozyme using sodium phosphate buffer. The steric factor for the proteins was obtained from a single non-linear frontal chromatographic experiment according to the expression:

$$\sigma_P = \frac{\beta}{C_P \Pi}\left[\Lambda - C_s\left(\frac{\Pi}{\beta K_P}\right)^{1/\nu_P}\right] - \nu_P \quad (13a)$$

where,

$$\Pi = \left(\frac{V_B}{V_0} - 1\right) \quad (13b)$$

In order to verify the model simulations, experimental isotherms of the proteins were also measured at several mobile phase salt conditions by frontal chromatography [13].

RESULTS AND DISCUSSION

In this paper, we present a simple experimental protocol for obtaining the SMA parameters required for simulating a wide range of displacement behavior. As described in the experimental section, a set of linear elution experiments along with one non-linear frontal experiment for the proteins, and two frontal experiments for the displacer, will yield sufficient information to determine all SMA parameters. In this paper, a rigorous evaluation of this parameter estimation protocol is carried out by comparing results from different techniques. Furthermore, the dependence of these parameters on mobile phase conditions and their relationship to the functional group density of the polyelectrolyte is investigated.

Bed capacity of ion exchangers

The total ion bed capacity for the anion-exchange column was determined *in situ* by a frontal experiment using sodium nitrate. These results were compared to capacities obtained by measuring the total amount of chloride ion displaced during the nitrate frontal experiment. As seen in Fig. 3A, there is excellent agreement between the values obtained from both methods. The bed capacities for the cation-exchange system were also determined at different salt concentrations (Fig. 3B). As seen in the figures, the bed capacities for both the anion- and cation-exchange systems were independent of the salt concentrations employed in the frontal experiments. Thus, a single frontal experiment is sufficient for the determination of total ion bed capacity. The ability to measure total ion bed capacity *in situ* facilitates SMA parameter estimation and enables a rapid test of column regeneration. As seen in Fig. 2, the superimposed initial and final nitrate breakthrough fronts confirm complete regeneration of the column from the adsorption of dextran sulphate molecules.

The bed capacity is reported here in molar units rather than equivalents. For a univalent ion the numerical value of bed capacity is the same in both units, since each ion binds to one site on the surface. The bed capacity of the cation exchanger for the divalent ions calcium and magnesium was independently measured, using the same frontal technique, to be 390 mM for each ion. Thus bed capacity for these divalent ions was not half of that for the sodium ion (561 mM) for the same adsorbent. This indicates that each divalent ion does not bind to exactly two sites on the surface due to morphological constraints. Clearly, a bed capacity expressed in mequiv. would be misleading in this case. In general, the use of mM units along with a specification of "characteristic charge" of the counter-ion is a more useful way of expressing bed capacity. In fact, mM units are required in order to develop a solute movement analysis of this model, as described in the subsequent paper.

Functional group density and characteristic charge of polyelectrolytes

While the determination of the characteristic charge and equilibrium constant from linear elution

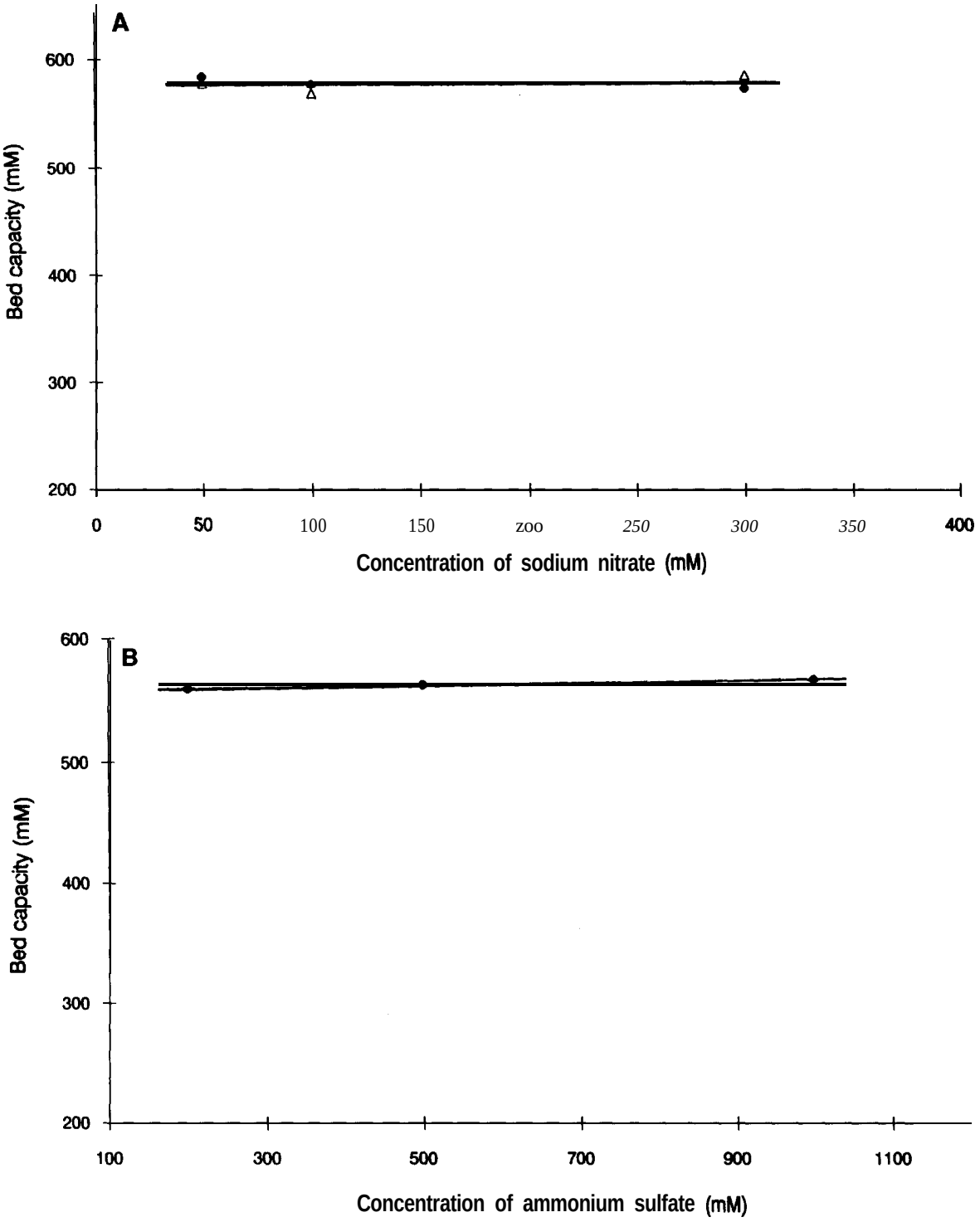

Fig. 3. Bed capacities of ion-exchange columns. (A) Anion-exchange column using the (△) nitrate and (●) chloride techniques; flow-rate: 0.25 ml/min; UV wavelength: 310 nm. (B) Cation-exchange column using ammonium sulphate; flow-rate: 0.5 ml/min.

data works well for moderately retained proteins, it is quite difficult to characterize high-molecular-mass polyelectrolyte displacers in this fashion due to their high affinity. Frontal chromatography, on the other hand, is well suited for parameter estimations for these high-affinity compounds.

Several frontal chromatographic methods were employed to determine both thecharacteristiccharge and steric factor of the displacers as described in the experimental section. Table I presents SMA parameters for dextran sulphate obtained with both the chloride- and nitrate-based techniques. As seen in the table, both techniques yielded essentially the same values. These results confirm the hypothesis that a front of nitrate ions, passed through a column saturated with the displacer, is able to access all the sterically hindered ion-exchange sites on the surface. Since these two methods are internally consistent, all future parameter estimations for anion-exchange systems can be carried out using the more convenient nitrate-based methods.

Parameter measurements for M_r 10 000 and 50 COO dextran sulphate displacers were carried out at various salt and polyelectrolyte concentrations to examine the effects of these operating conditions on the SMA parameters. These studies employed moderate mobile phase salt concentrations, typically used for the displacement experiments. As seen in Table I, both the characteristic charge and the steric factors were essentially independent of mobile phase salt and displacer concentration. The characteristic charge of these polyelectrolytes was invariant even when the mobile phase salt concentration was increased 5 to 10 fold. Similarly, the steric factor was observed to be independent of the mobile phase salt and displacer concentration. These results are significant in that they indicate, for these high affinity displacers, that the measurement of these parameters under a single set of mobile phase conditions is sufficient to predict their adsorption behavior for a range of mobile phase conditions. The characteristic charge and steric factor of DEAE-dextran displacers in the cation-exchange system were also found to be insensitive to the mobile phase salt and displacer concentrations.

Fig. 4a and b shows the induced salt gradient produced by the adsorption of the displacers at various salt and solute concentrations. As seen in the figure, the induced salt gradient for each displacer increased linearly with the displacer concentration.

TABLE I

CHARACTERISTIC CHARGE AND STERIC FACTOR OF DEXTRAN SULPHATES: COMPARISON OF TECHNIQUES

Chromatographic conditions: SAX column; buffer: tris chloride, pH 7.5; ion bed capacity = 567 mM.

M_r	Salt concentration (mM)	Dextran sulphate concentration (mM)	$\nu_{D,chloride}$ [a]	$\nu_{D,nitrate}$ [b]	$\sigma_{D,chloride}$ [c]	$\sigma_{D,nitrate}$ [d]
10 000	50	0.5	33.8	32.3	33.12	34.8
10000	50	1	31.3	29.2	34.5	33.6
10 000	100	0.5	30.2	32.4	32.2	34.2
10 000	100	1	32.1	31.0	32.2	32.1
10 000	100	2	32.3	32.5	34.0	33.2
10 000	250	1	N.D.	31.1	N.D.	33.4
50 000	50	0.2	152.3	145.7	160.0	166.7
50 000	50	0.4	144	145.1	169.7	165.3
50 000	100	0.2	140.9	141.6	160.1	161.8
50 000	100	0.4	137.4	137.2	161.3	165.1
50 000	500	0.4	N.D.	135.9	N.D.	167.1

[a] Defined in eqn. 3.
[b] Defined in eqn. 7.
[c] Defined in eqn. 6.
[d] Defined in eqn. 5.

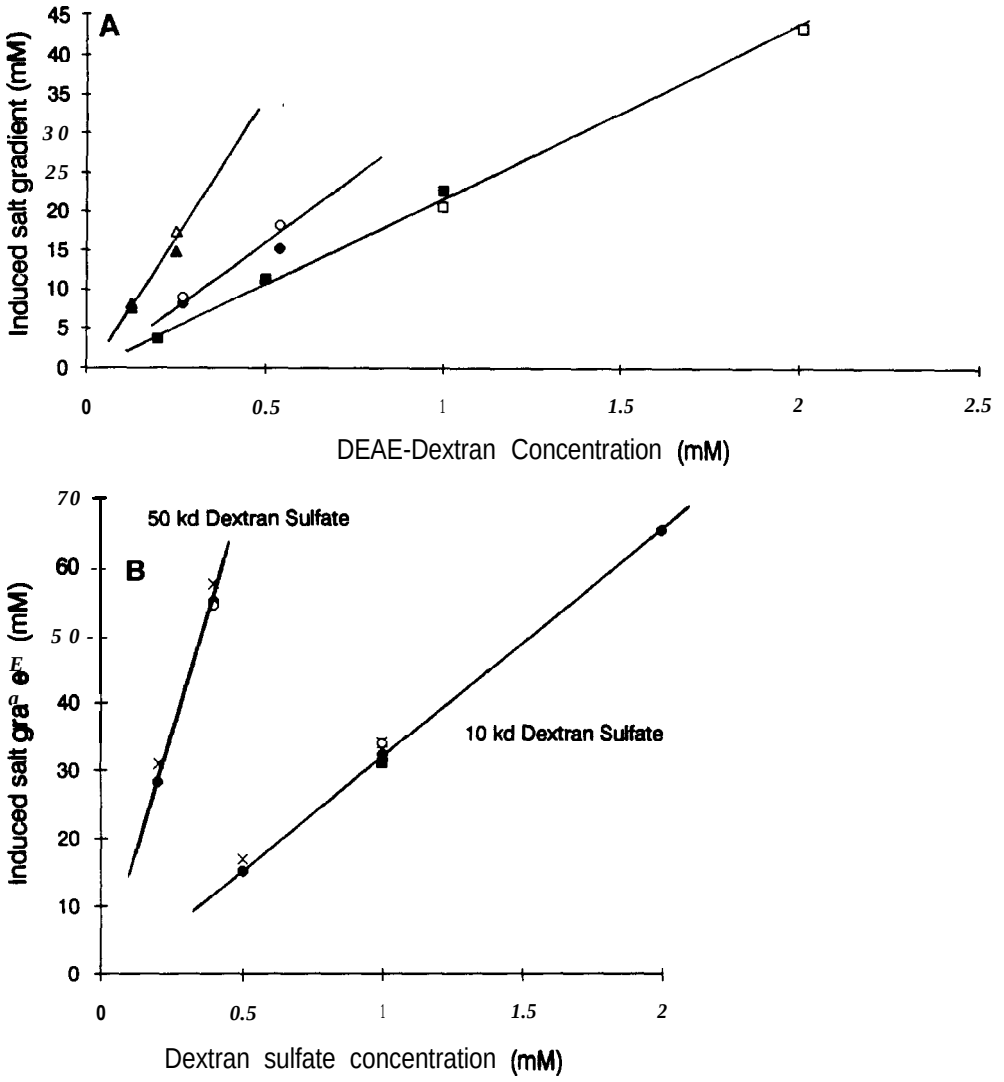

Fig. 4. Induced salt gradients as a function of inlet displacer concentration in ion-exchange systems. (A) M_r 10 000 (□, ■), 20 000 (○, ●) and 40 000 (△, ▲) DEAE–dextran in cation-exchange system; closed symbols at 20 m*M* Na^+; open symbols at 75 m*M* Na^+, pH 6.0; flow-rate: 0.2 ml/min; detection: RI. (B) Dextran sulphate (10 000 and 50 000) in anion-exchange system at (×) 50, (●) 100, (■) 250 and (○) 500 m*M* Cl^-, pH 7.5; flow-rate: 0.2 ml/min; detection: UV 252 nm. kd = kilodalton.

The average characteristic charge of the polyelectrolyte displacers can be obtained directly from the slope of these lines and are presented in Table II.

Data obtained from the elemental analyses was employed to calculate the functional group density and the number of functional groups in each polyelectrolyte. As expected, higher-molecular-mass displacers possess correspondingly higher numbers of functional groups and characteristic charges. The dextran sulphates have a greater degree of functionalization than the DEAE-dextran materials. The characteristic charge and functional group results are also presented in normalized form (i.e., per repeating unit of the polymer). The repeating unit employed in these calculations was the disaccharide [14]. While the functional group density of

TABLE II

CHARACTERISTIC CHARGE AND FUNCTIONAL GROUP DENSITY OF DEXTRAN POLYELECTROLYTES

Displacer	Elemental analyses (%, w/w)	Functional group density[a]	Number of functional groups (f)	Characteristic charge (ν_D)	Normalized characteristic charge[b]	Fraction of groups bound (ν_D/f)
10 000 Dextran sulphate	16.0% S	2.67	59	31	1.65	0.62
50 000 Dextran sulphate	16.3% S	2.17	255	140	1.52	0.55
10 000 DEAE-dextran	3.1% N	1.15	26	21	0.91	0.81
20 000 DEAE-dextran	2.8% N	0.81	40	31	0.62	0.78
40 000 DEAE-dextran	3.5% N	1.08	100	64	0.69	0.64

[a] Functional group density is defined as the average number of functional groups per repeating unit of the polyelectrolyte.
[b] Normalized characteristic charge is defined as the characteristic charge per repeating unit of the polyelectrolyte.

each class of dextran-based polyelectrolytes was essentially constant (with the exception of the M_r 20 000 DEAE-dextran), the normalized characteristic charge decreased with molecular mass. In other words, a relatively smaller fraction of the total number of functional groups is bound for higher-molecular-mass polyelectrolytes. This effect is the most striking for the DEAE–dextran materials. In fact, this change in normalized characteristic charge with molecular mass is a reflection of different conformations of these polyelectrolytes in the adsorbed state. It is likely that, an increase in molecular mass is associated with an increase in the relative amounts of loops and tails in the adsorbed polyelectrolyte.

Steric factor of polyelectrolytes

Table III presents the average values of the steric factors for dextran sulphates and DEAE dextrans of various molecular masses. For all polyelectrolytes, the values of the steric factors were comparable to the characteristic charges. These results indicate that a significant portion of the adsorption sites on the chromatographic surface are sterically blocked by the polyelectrolytes and are not available for exchange with unbound polyelectrolytes solutes. The characteristic charge and the steric factor of these linear polyelectrolytes depends on the number of functional groups on the polyelectrolyte and their positioning relative to the exchange sites on the adsorption surface. Table III also indicates that the ratio of steric factor to characteristic charge increased with molecular mass. This effect is more pronounced for the DEAE–dextrans. This is due to a combination of lower normalized characteristic charge and relatively less dense surface coverage for higher-molecular-mass polyelectrolytes.

It is important to note that the steric factor reported in this manuscript represents the salt counter-ions which are "unavailable" for exchange with other macromolecules. In practice, this parameter may also include size-exclusion effects. How-

TABLE III

AVERAGE VALUES OF SMA PARAMETERS FOR DEXTRAN DISPLACERS

Displacer	Characteristic charge (ν_D)	Steric factor (σ_D)	(σ_D/ν_D)	Q_D^{max} (mM)	$Q_D^{max} \cdot \nu_D$ (mequiv.)
10 000 Dextran sulphate	31	33	1.06	9.11	282
50 000 Dextran sulphate	140	162	1.16	1.87	260
10 000 DEAE-dextran	21	32	1.52	10.66	223
40 000 DEAE-dextran	64	130	2.03	3.08	196

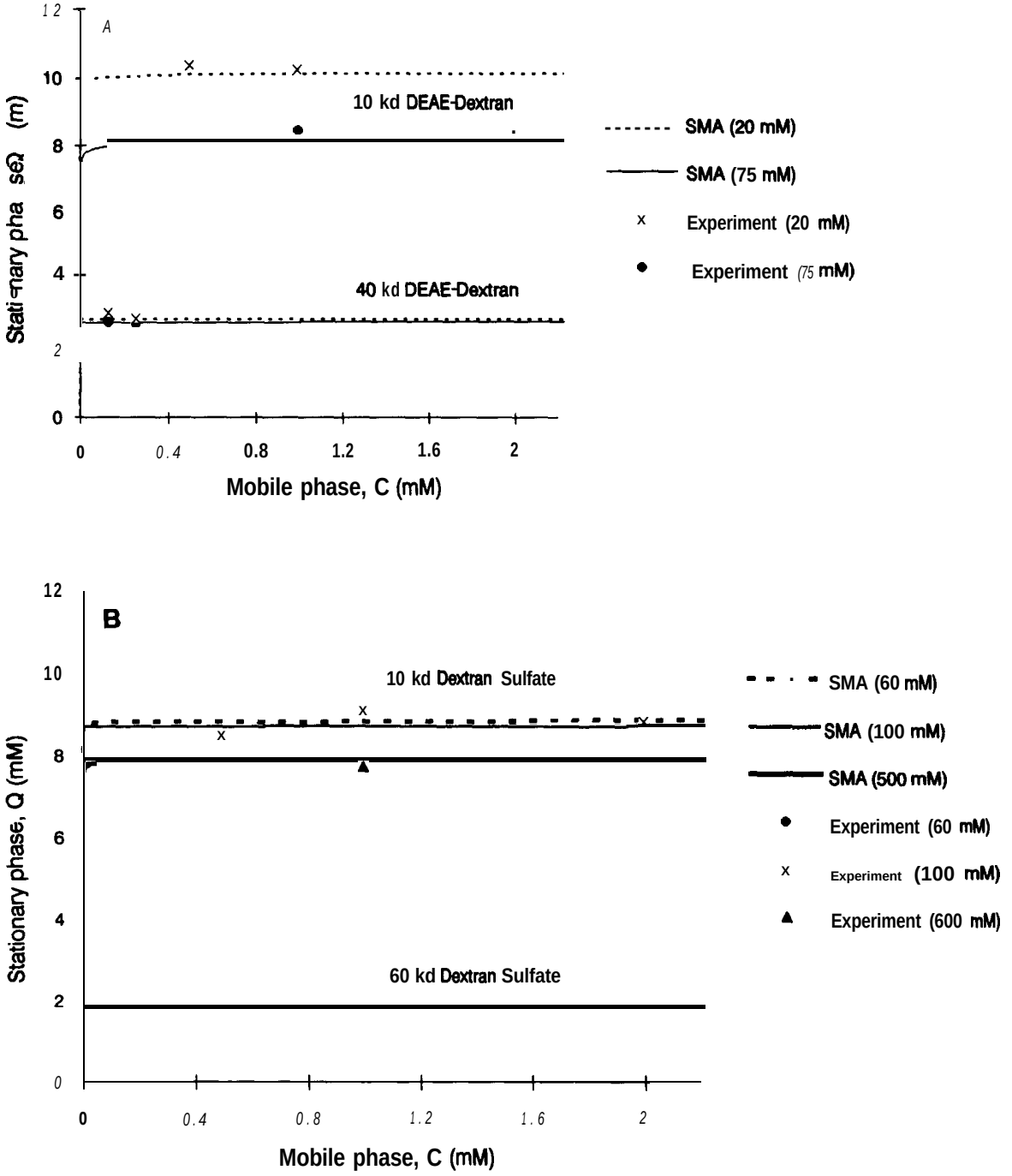

Fig. 5. Experimental and SMA isotherms of (A) DEAE–dextran; mobile phase: sodium phosphate, pH 6.0; detection: RI and (B) dextran sulphate; mobile phase: Tris–HCl, pH 7.5; flow-rate: 0.2 ml/min; detection: UV 252 nm.

ever, chromatographic analysis of the macromolecules under unretained conditions indicated no measurable size-exclusion effects in these columns.

The affinity of binding of a polyelectrolyte increased with molecular mass due to a corresponding increase in its characteristic charge. Conversely, the maximum molar binding capacity (Q^{max}) decreased with increase in molecular mass as shown in Table III. The product of the stationary phase concentration of the polyelectrolyte and its characteristic charge ($Q^{max} \cdot \nu$) is a measure of the total number of interactions between the adsorbed polyelectrolyte and the adsorbent surface under the saturation conditions. For higher-molecular-mass polyelectrolytes, a correspondingly smaller number of total bonds are formed with the surface, due to their greater steric factor.

Equilibrium adsorption constant of polyelectrolytes

Once the characteristic charge and steric factor are measured independently, the equilibrium adsorption constant can be calculated from a frontal experiment under non-saturating conditions using eqn. 11. However, the value of K can only be determined for molecules which demonstrate salt-dependent adsorption behavior. In practice, this is quite difficult for the higher-molecular-mass displacers since their Q values exhibit very little or no dependence on the mobile phase salt concentration. M_r 50 000 dextran sulphate exhibited maximum saturation at all salt concentrations used in the experiments. Accordingly, a sufficiently high value of K was employed in the isotherm simulations. While a K value was obtained for the M_r 40 000 DEAE–dextran ($K = 5.45 \cdot 10^{44}$), this value is only approximate due to the weak salt dependence of the polyelectrolyte. On the other hand, the smaller displacers (M_r10 000 dextran sulphate, 10 000 DEAE–dextran) exhibited significant salt-dependent adsorption behavior. The K values for the M_r 10 000 dextran sulphate and DEAE–dextran displacers were determined to be $3.6 \cdot 10^{28}$ and 0.0063, respectively. It is important to note that the equilibrium constant in the SMA formalism is defined differently from the conventional Henry's law constant. This wide range of values is due to the exponential dependence of K on characteristic charge (eqn. 3) and the fact that the equilibrium constant K is unique for each ion-exchange equilibria.

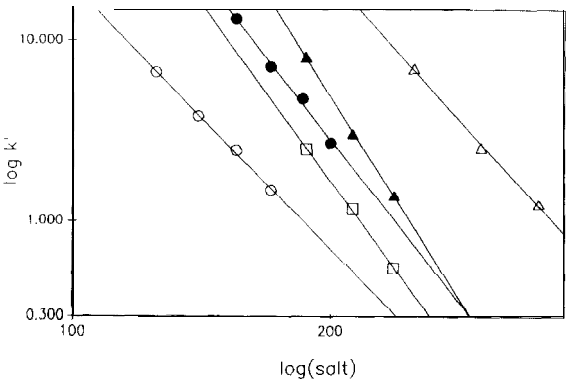

Fig. 6. Linear elution data for the determination of protein characteristic charge and equilibrium adsorption constant. Chromatographic conditions: for anion-exchange proteins [(A) β-lactoglobulin A and B, (□) β-lactoglobulin B]; mobile phase: Tris-HCI, pH 7.5; for cation-exchange proteins [(0) α-chymotrypsinogen, (●) cytochrome c and (△) lysozyme]; mobile phase: sodium phosphate, pH 6.0.

Isotherms of polyelectrolytes

Once the characteristic charge, steric factor and equilibrium constants are determined, the isotherms of the polyelectrolytes can be simulated using the SMA formalism of Brooks and Cramer [IO]. The experimentally measured isotherms of the polyelectrolytes were compared with the simulated isotherms in Fig. 5.

These results confirm the square nature of the polyelectrolyte equilibrium isotherms under different mobile phase salt concentrations [2,3,15]. Since these polyelectrolytes approach square isotherms,

TABLE IV

SMA PARAMETERS FOR PROTEINS

Chromatographic conditions: β-lactoglobulin A and B: SAX column, Tris buffer, pH 7.5; other proteins: SCX column, sodium phosphate buffer, pH 6.0.

Protein	Characteristic charge (ν_P)	Steric factor (σ_P)	Equilibrium constant (K_P)
a-Chymotrypsinogen	4.8	49.2	9.22. IO-'
Cytochrome c	6.0	53.6	$1.06 \cdot 10^{-2}$
Lysozyme	5.3	34.0	1.84. IO-'
β-Lactoglobulin A	7.5	38.2	$5.44\ 10^{-3}$
β-Lactoglobulin B	6.3	41.5	$6.42.\ 10^{-3}$

measurements need only be carried out at one or two polyelectrolyte mobile phase concentrations. As seen in the figures, the equilibrium binding capacity (Q) of higher-molecular-mass polyelectrolytes is essentially independent of the mobile phase salt concentration. On the other hand, the lower-molecular-mass polyelectrolytes (10 000) display some variance in their binding capacities with mobile phase salt concentration. Salt counter-ions compete more effectively for adsorption sites with lower-molecular-mass polyelectrolytes having a relatively smaller number of bonds with the surface. The

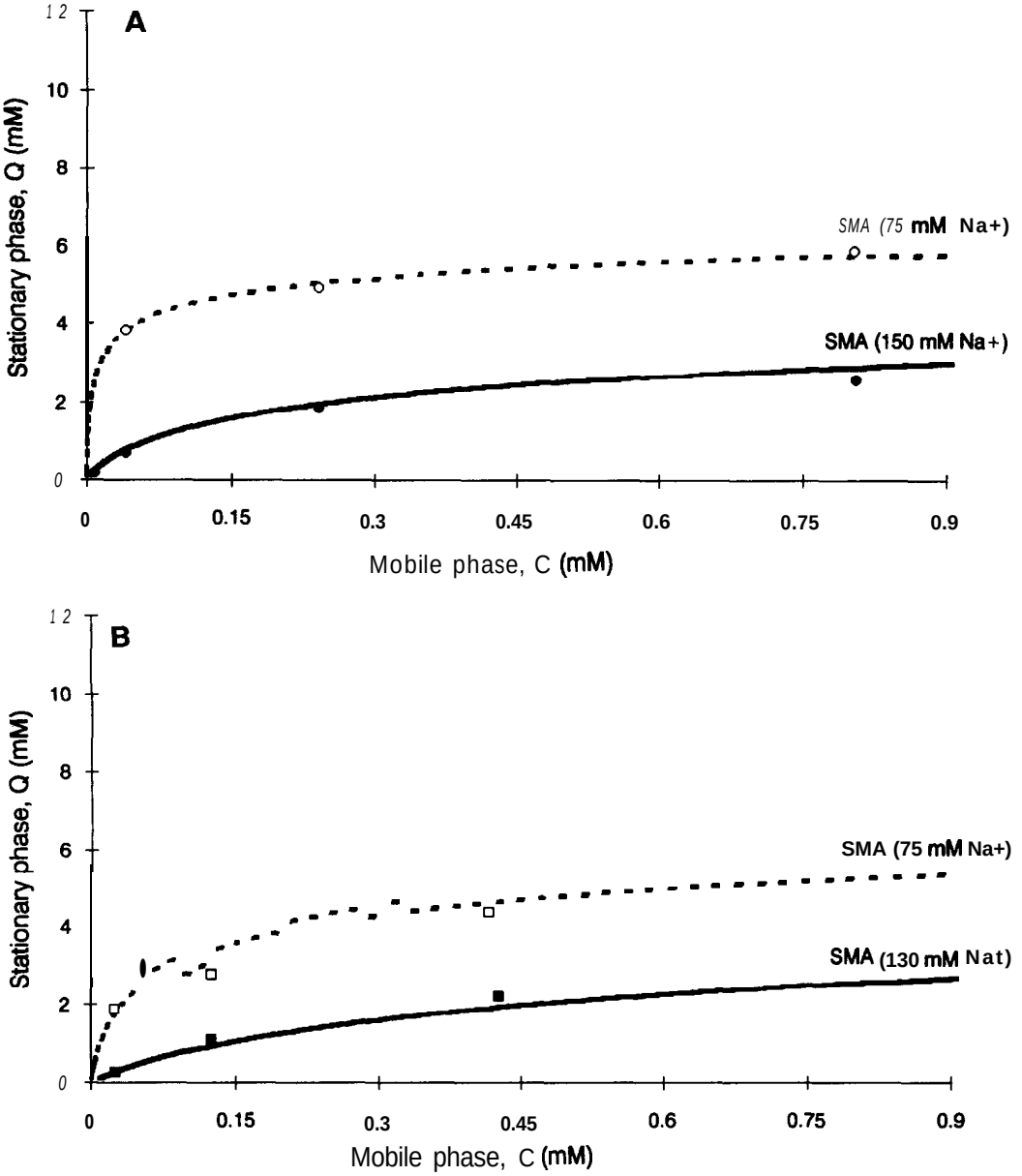

Fig. 7. Experimental and SMA isotherms of (A) cytochrome *c* at (0) 75 m*M* and (●) 150 m*M* sodium phosphate, pH 6.0; (B) a-chymotrypsinogen at (□) 75 m*M* and (■) 130 m*M* sodium phosphate, pH 6.0.

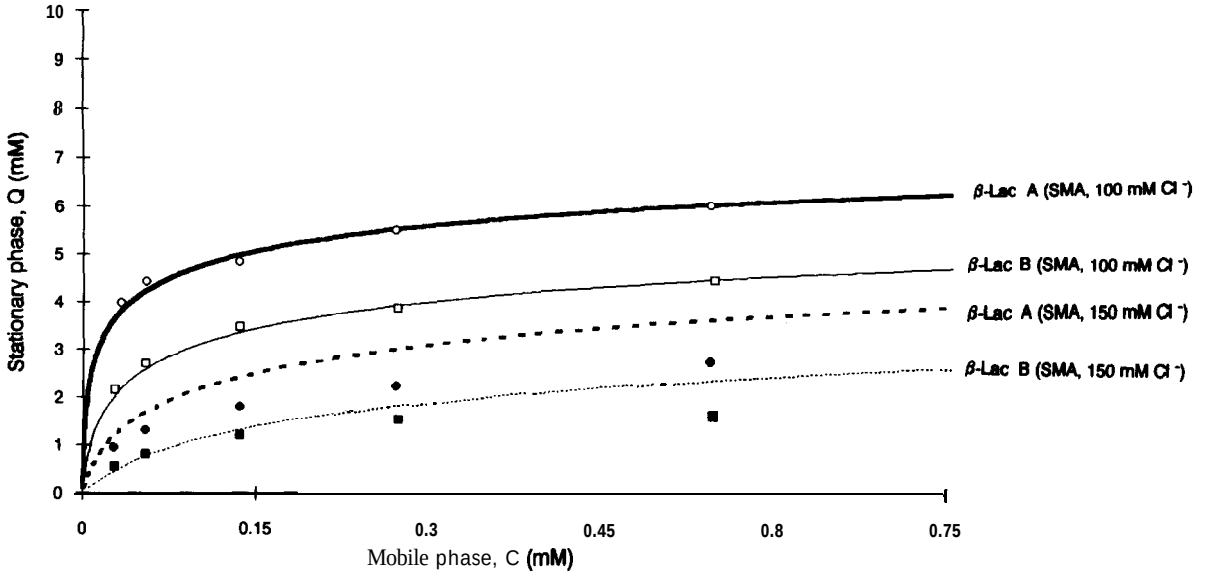

Fig. 8. Experimental and SMA isotherms of β-lactoglobulin A and B at 100 m*M* (open symbols) and 150 m*M* (closed symbols); mobile phase: Tris–HCl, pH 7.5

weaker salt dependence of the polyelectrolyte isotherms as compared to the protein isotherms lends significant flexibility for design of displacement chromatographic separation of proteins.

SMA parameters of proteins

The characteristic charge and equilibrium constant for several model proteins were obtained using the linear elution method described in the experimental section. As seen in Fig. 6, all measured proteins exhibited linear ln k' plots. The steric factors of the proteins were determined using the non-linear frontal chromatographic technique in concert with eqn. 13. The resulting SMA parameters for these proteins are presented in Table IV. In contrast to the results described above for the dextran-based displacers, the proteins exhibited significantly higher steric factors relative to their characteristic charge. This is not surprising in light of the conformational constraints in the protein molecules.

Once the SMA parameters are obtained for a given protein, the model can then be used to generate adsorption isotherms at any salt concentration. Clearly, an important test of the SMA formalism is a comparison between theoretical and experimentally determined isotherms. Adsorption isotherms of the proteins cytochrome c and cc-chymotrypsinogen A are presented in Fig. 7. These results confirm that the SMA formalism is well suited for describing protein adsorption behavior at various salt conditions. In contrast, the isotherms for β-lactoglobulin A and B (Fig. 8) are not as well described by the SMA formalism. There are several possible explanations for this deviation from "ideal" SMA behavior. These include: aggregation [16–18], as well as salt-dependent changes in the adsorbed protein conformation. These phenomena are currently under active investigation in our laboratory.

CONCLUSIONS

Frontal chromatography offers a useful technique for characterizing the adsorption behavior of high-affinity polyelectrolytes. The experimental techniques presented in this paper not only enable us to measure the SMA parameters but also provide a powerful tool to evaluate the efficacy of polyelectrolytes as displacers for ion-exchange protein separations.

The physico-chemical properties (e.g., functional group density and molecular mass) of the polyelec-

trolytes will have a profound effect on their efficacy as a displacer for ion-exchange protein separations. For a given functional group density of the polyelectrolyte and ligand distribution of the adsorbent surface, adsorption of higher-molecular-mass polyelectrolyte is associated with a decrease in normalized characteristic charge and a corresponding increase in the steric factor. For a given molecular mass, a higher density of functional groups on the polyelectrolyte will result in a higher characteristic charge and lower steric factor with a concomitant increase in the induced salt gradient. Thus, by manipulating the functional group density and molecular mass of the polyelectrolyte, one can control the affinity of the molecule as well as the induced salt gradients. Furthermore, the density of ion-exchange sites on the chromatographic surface will directly influence the characteristic charge and steric factor of the polyelectrolyte. In the subsequent manuscript we will examine these effects with respect to the ion-exchange displacement separation of proteins.

These parameter estimation protocols in concert with the SMA formalism establish a powerful framework for rational design of efficient displacers for ion-exchange systems. Extension of these studies to a variety of polyelectrolyte compounds will lead to a formulation of generalized rules of thumb relating the polyelectrolyte structure to their adsorption behavior.

SYMBOLS

All mobile phase concentrations are defined per unit volume of mobile phase. All stationary phase concentrations and the bed capacities are defined per unit volume of stationary phase.

C_D	Concentration of polyelectrolyte in the mobile phase (mM)
$C_{nitrate}$	Concentration of the nitrate front in the mobile phase (mM)
C_P	Concentration of protein in the mobile phase (mM)
C_s	Salt concentration in the carrier (mM)
ΔC_s	Step increase in the mobile phase salt concentration upon displacer adsorption (mM)
k	Dimensionless retention time of proteins
K_D	Equilibrium constant of polyelectrolyte displacers
K_P	Equilibrium constant of proteins
n_1	Salt displaced by displacer front (mmol)
n_2	Salt displaced by nitrate front (mmol)
n_D	Displacer adsorbed on the stationary phase (mmol)
Q_D	Stationary phase concentration of the displacer (mM)
Q_D^{max}	Maximum binding capacity of the polyelectrolyte on the stationary phase (mM)
$\bar{Q}_s$	Stationary phase concentration of sterically unhindered salt (mM)
V_0	Dead volume of the column (ml)
V_B	Breakthrough volume of displacer front (ml)
$V_{B\text{-nitrate}}$	Breakthrough volume of nitrate front (ml)
V_{sp}	Column stationary phase volume (ml)

Greek letters

β	Column phase ratio
Λ	Ion bed capacity (mM)
ν_P	Characteristic charge of proteins
$\nu_{D,chloride}$	Characteristic charge of the displacer based on chloride method defined in eqn. 6
$\nu_{D,nitrate}$	Characteristic charge of the displacer based on nitrate method defined in eqn. 10
σ_P	Steric factor of proteins
$\sigma_{D,chloride}$	Steric factor of the displacer based on chloride method defined in eqn. 9
$\sigma_{D,nitrate}$	Steric factor of the displacer based on nitrate method defined in eqn. 8

ACKNOWLEDGEMENTS

This research was funded by Millipore Corporation and grants BCS-9112481 and CTS-8957746 (a Presidential Young Investigator Award to S. M. Cramer) from the National Science Foundation. Chromatographic materials and equipment were donated by Millipore Corporation (Waters Chromatography Division, Millipore, Milford, MA, USA). The dextran derivatives were donated by Pharmacia-LKB Biotechnology. The authors acknowledge Professor Joyce Diwan (Department of Biology, Rensselaer Polytechnic Institute) for use of the atomic absorption spectrophotometer.

REFERENCES

1 H. A. van der Schee and J. Lyklema, *J. Phys. Chem., 88* (1984) *6661.*
2 J. Papenhuyzen, H. A. van der Schee and G. J. Fleer, *J.* Colloid ***Interface Sci.,*** 104 (1985) 553.
3 0. A. Evers, G. J. Fleer, J. M. H. M. Scheutjens and J. Lyklema, ***J. Colloid Interface Sci.,*** 111 (1986) 446.
4 R. J. Roe, ***J. Chem.*** *Phys.*, ***60*** (1974) ***4192.***
5 J. M. H. M. Scheutjens and G. J. Fleer, *J. Phys.* Chem., 83 (1979) 1619.
6 J. M. H. M. Scheutjens and G. J. Fleer, ***J. Phys.*** Chem., 84 (1980) 178.
7 E. A. Peterson, ***Anal. Biochem., 90 (1978) 767.***
8 E. A. Peterson and A. R. Torres, ***Anal. Biochem., 130 (1983) 271.***
9 S. ***C.*** D. Jen and N. G. Pinto, ***J. Chromatogr.*** *Sci.*, ***29*** (1991) 1.
10 C. A. Brooks and S. M. Cramer, *AIChE J.*, ***38 (12) (1992) 1969.***
11 ***Standard Test Methods for Chloride Ion in Water, Annual Book of ASTM Standards,*** Vol. 11.01, ASTM, Philadelphia. PA, 1991.
12 D. Bentrop and H. Engelhardt, ***J. Chromatogr., 556*** (1991) 363.
13 J. Jacobson, J. Frenz and Cs. Horváth, ***J. Chromatogr., 316 (1988) 53.***
14 K. G. Ludwig-Baxter, R. N. Rej, A. S. Perlin and G. A. Neville, ***J. Pharm. Sci., 80 (7)*** 1991.
15 J. Blaakmeer, M. R. Bohmer, M. A. Cohen Stuart and G. J. Fleer, ***Macromolecules, 23*** (1990) ***230***1.
16 H. A. McKenzie, in H. A. McKenzie (Editor), *Milk* ***Proteins. Chemistry and Molecular*** *Biology*, Vol. ***2,*** Academic Press, New York, 1971. Ch. 14.
17 R. D. Whitley, K. E. Cott, J. A. Berninger and N.-H. L. Wang. *AIChE J.*, ***37 (4) (1991) 555.***
18 ***N.*** Grinberg, R. Blanco, D. M. Yarmush and B. L. Karger, ***Anal.*** *Chem.*, ***61 (6) (1989) 515.***